

Brine transport in porous media: self-similar solutions

C.J. van Duijn^a, L.A. Peletier^b & R.J. Schotting^{c,*}

^aP.O. Box 94079, 1090 GB Amsterdam, The Netherlands

^bMathematical Institute, Leiden University, P.O. Box 9512, 2300 RA Leiden, The Netherlands

^cDepartment of Watermanagement, Environmental and Sanitary Engineering, Delft University of Technology, P.O. Box 5048, 2600 GA Delft, The Netherlands

(Received 28 October 1996; revised 10 March 1998; accepted 20 March 1998)

In this paper we analyze a model for brine transport in porous media, which includes a mass balance for the fluid, a mass balance for salt, Darcy's law and an equation of state, which relates the fluid density to the salt mass fraction. This model incorporates the effect of local volume changes due to variations in the salt concentration. Density variations affect the compressibility of the fluid, which in turn cause additional fluid flow. Two specific situations are investigated that lead to self-similarity. We study the relative importance of the compressibility effect in terms of the relative density difference. Semi-analytical solutions are obtained as well as asymptotic expressions in terms of the relative density difference. It is found that the volume changes have a small but noticeable effect on the mass transport only when the salt concentration gradients are large. Some results on the simultaneous transport of brine and dissolved (radioactive) tracers are presented. © 1998 Elsevier Science Limited. All rights reserved

Keywords: brine transport, compressibility, similarity transformations, porous media, 35K55, 76S05.

1 INTRODUCTION

Recently Hassanizadeh and Leijnse^{1–3} revisited the theory of brine transport in porous media, designed numerical codes and did experiments in the laboratory. They raised the question whether (semi-) analytical solutions of the governing equations could be obtained under certain boundary and initial conditions. This question initiated our mathematical study and the results are published in the mathematics literature⁴. Because the subject of brine transport is still of current interest in the hydrological literature and the availability of analytical work in this field is poor, we decided to make the mathematical results more accessible for non-mathematicians and wrote this paper. The material has been extended with new results and the emphasis is now on the construction of semi-explicit self similar solutions.

Brine is water containing a high concentration of salt. In an almost saturated brine the *mass fraction* (ω), which is

defined as the mass of the salt per unit mass of brine, can reach 0.26. This corresponds to a brine density of approximately 1200 kg m^{-3} . For sea water $\omega = 0.04$ corresponding to a fluid density of 1025 kg m^{-3} . Mass fraction and density are related by an equation of state, which has been empirically determined. Brines are found in surface waters, such as the Dead Sea, and groundwater near salt domes⁵. These are geological structures in the subsurface consisting of massive bodies of salt, a kilometer or more in diameter, embedded in horizontal or inclined strata. Salt domes are potential places for storage of nuclear waste⁶, and it is of practical importance to know the flow of the groundwater around them.

Any model for fluid flow and salt transport in a porous medium must contain the mass balance equations for the fluid and the salt, and Darcy's law. The specific model we propose to study uses the fluid mass balance equation¹

$$\phi \frac{\partial \rho}{\partial t} + \text{div}(\rho \mathbf{q}) = 0 \quad (1)$$

where ϕ denotes the porosity of the medium, ρ the fluid density and \mathbf{q} the specific discharge vector. Introducing the

*Corresponding author. Tel: 0031 15 278 1692; Fax: 0031 15 278 7209; e-mail: r.j.schotting@twi.tudelft.nl

material derivative

$$\frac{D}{Dt} = \frac{\partial}{\partial t} + \frac{\mathbf{q}}{\phi} \cdot \text{grad} \tag{2}$$

in the balance equation yields

$$\frac{\phi}{\rho} \frac{D\rho}{Dt} + \text{div} \mathbf{q} = 0 \tag{3}$$

This expression shows that density variations may affect the compressibility of the fluid, which in turn can affect the fluid motion. To make this effect explicit is one of the goals of this study.

In this paper we intend to employ mainly analytical techniques. Therefore, we are forced to restrict ourselves in the choice of flow problems. Inspired by earlier work of de Josseling de Jong and van Duijn⁷ we shall analyze two simplified cases denoted by Problem I and Problem II. Problem I describes the mixing of fresh water and brine, originally separated and flowing parallel, due to transversal dispersion. Problem II relates to the flow of groundwater along the surface of a salt dome. A sketch of the corresponding initial and boundary conditions is given in Fig. 1. In Problem I the flow domain is unbounded above and below. Initially, say at $t = 0$, the region above the plane $\{z = 0\}$ is filled with fresh water and the brine fills the region below it. In this case one has to specify the specific discharge either as $z \rightarrow +\infty$ or as $z \rightarrow -\infty$. Here we shall adopt the former, and fix $\mathbf{q} \rightarrow (q_f, 0)$ as $z \rightarrow +\infty$, where q_f is a given constant. In Problem II the flow domain consists of the upper half space $\{z > 0\}$ and is bounded below by an impermeable salt rock. Again at $t = 0$, fresh water occupies the region $\{z > 0\}$ while the salt from the rock ensures that $\rho = \rho_s$ (mass density of saturated brine) along the boundary $\{z = 0\}$. Here we can only specify the y -component of the specific discharge at $z = +\infty$, because the z -component is determined by a second boundary condition, as explained in Section 3, at the surface of the rock. In both problems the y -coordinate ranges from $-\infty$ to $+\infty$. Moreover, only stable displacement of salt is considered, implying $-\pi/2 < \beta < +\pi/2$.

These problems are chosen because they admit to look for similarity solutions. This means that the underlying partial differential equations can be reduced to ordinary differential equations by introducing an appropriate similarity variable (e.g. z/\sqrt{t} in Fig. 1). This makes the analysis tractable, yielding semi-explicit results. The mathematical justification of the results is given elsewhere⁴. As a consequence of the analysis we can quantify the effect of the additional brine transport due to the fluid compressibility for Problems I and II, where in particular the latter is relevant to understand the flow near salt domes.

Among recent papers focusing on brine transport we mention Oldenburg and Pruess⁸; Carey et al.⁹, Herbert et al.¹⁰, Hassanizadeh and Leijnse³. Numerical codes^{1,2} are developed to simulate flow of groundwater containing high salt concentrations. There are only few high-concentration brine transport experiments available for testing the validity of numerical codes. Our (semi) analytical results can be used to verify the accuracy of numerical codes^{11,2}. Herbert et al.¹⁰ stresses the importance of analytical work on this subject.

In the literature, the validity of Darcy's law and Fickian dispersion equations for high concentration differences has been questioned. For example, Hassanizadeh and Leijnse³ reported on column tests of brine displacing fresh water in a porous medium. They showed that the dispersivity of brine decreases when the relative density difference between brine and fresh water increases and resolved this problem by introducing a non-linear form of Fick's law. Carey et al.⁹ suggest a density dependent diffusivity–dispersivity. Although these results are interesting we shall confine ourselves to the classical formulation of Fick's and Darcy's law in this paper.

In Section 2 we formulate the mathematical model in general terms and in Section 3 we define the two specific problems I and II. Dimensionless variables are introduced in Section 4. In Section 5 we discuss properties and construction of self-similar solutions. Numerical procedures and results are given in Section 6 while asymptotic results for

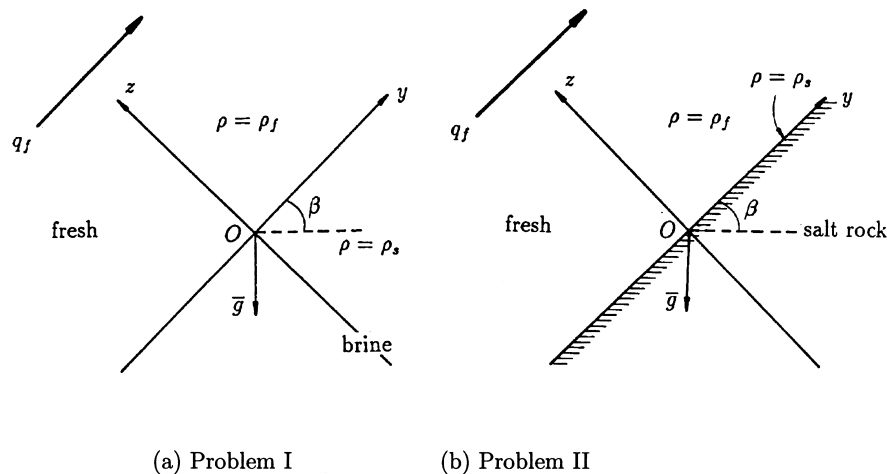


Fig. 1. Initial and boundary conditions.

small relative density difference, yielding approximately $\text{div}(\mathbf{q}) = 0$, can be found in Section 7. The simultaneous transport of brine and dissolved radionuclides is the subject of Section 7. In Section 8 we discuss the results and Section 9 contains the conclusions.

2 THE MATHEMATICAL MODEL

Since this paper focuses on analytical aspects of subsurface brine transport, we shall impose simplifying restrictions on the properties of the porous medium and flow. With respect to the porous medium we assume that it is homogeneous and isotropic, characterized by a constant porosity ϕ and intrinsic permeability κ . With respect to the flow we shall consider the two specific cases which are introduced in Section 1 and about the fluid, with density ρ and salt mass fraction ω , we assume that the dynamic viscosity μ does not depend on ω and is constant.

Assuming a Fickian type of dispersion–diffusion term in the salt mass flux and restricting ourselves to the conventional form of the momentum balance equation, we obtain the following equations for transport of brine¹:

Mass balance of the fluid

$$\phi \frac{\partial \rho}{\partial t} + \text{div}(\rho \mathbf{q}) = 0; \quad (4)$$

Mass balance of the salt

$$\phi \frac{\partial \rho \omega}{\partial t} + \text{div}(\rho \omega \mathbf{q}) - D \rho \text{grad} \omega = 0; \quad (5)$$

Darcy's law

$$\frac{\mu}{\kappa} \mathbf{q} + \text{grad} p - \rho \mathbf{g} = 0; \quad (6)$$

Equation of state

$$\rho = \rho_f e^{\gamma \omega} \quad (7)$$

Here $\mathbf{q} = (q_y, q_z)$ denotes the specific discharge, p the fluid pressure and $\mathbf{g} = (g_y, g_z)$ the acceleration of gravity. In the equation of state, where we disregard the effect of pressure variations on the fluid density, ρ_f is the density of the fresh water and γ is a constant ($\gamma = 0.6923 \approx \ln 2$) obtained by curve fitting using a table from Weast¹². Following Bear¹³, the hydrodynamic dispersion tensor $\mathbf{D} = (D_{ij})$ is given by the expression

$$D_{ij} = \{\alpha_T |\mathbf{q}| + \phi D_{mol}\} \delta_{ij} + (\alpha_L - \alpha_T) q_i q_j / |\mathbf{q}| \quad (8)$$

where α_L and α_T are positive constants with $\alpha_L > \alpha_T$. They are called the longitudinal and transversal dispersion length, and describe the spreading of solutes due to mechanical dispersion caused by randomness of the structure of the porous material and heterogeneities. Further D_{mol} denotes the effective molecular diffusivity, which incorporates the effect of tortuosity. Finally, δ_{ij} denotes the Kronecker δ and $|\cdot|$ the Euclidian norm in \mathbf{R}^2 . For

mathematical reasons we use in most of this paper (except in Section 9) the approximation

$$D_{ij} = \phi D \delta_{ij} \quad (9)$$

where D is a positive constant.

3 THE FLOW PROBLEMS

The object of any study of brine transport is to determine the specific discharge and density (or mass fraction of salt) of the fluid as a function of position and time. We will investigate here two specific problems. In Problem I, see Fig. 1(a), we consider an unbounded flow domain above and below the $z = 0$ plane. Initially, at time $t = 0$ say, the region above this plane is filled with fresh water (density ρ_f) and the region below it with brine (density ρ_s). Since $\rho_s > \rho_f$ and assuming $-\pi/2 < \beta < +\pi/2$, this leads to a stable salt distribution for all $t \geq 0$. As a boundary condition we impose that at large distance above the $z = 0$ plane, the flow is known (and given) and points into the y -direction:

$$\mathbf{q} \rightarrow q_f \mathbf{e}_y \text{ as } z \rightarrow +\infty, \text{ for all } t \geq 0 \quad (10)$$

where q_f is a given constant and \mathbf{e}_y the unit vector in the positive y -direction.

Studies of brine distributions in aquifers have shown that the transition zone between brine and fresh water is relatively narrow, in particular when the fluids are stagnant. If this situation is perturbed by draining fresh water we end up with a situation that can be represented schematically by Problem I.

In Problem II the flow domain occupies the half space $\{z > 0\}$, see Fig. 1(b). In formulating this problem we have assumed the initial situation where, due to regional effects, fresh groundwater flows along the top boundary of a salt dome. As a result salt will dissolve from it. The physico-chemical processes that take place at a salt rock boundary are complex and difficult to model. For instance, the dissolution of salt creates a cap (residue) rock layer along the top of the salt dome. Geological studies, e.g. Bornemann et al.¹⁴, estimate the growth of this layer to be $0.04 \text{ mm year}^{-1}$. Following Hassanizadeh and Leijnse¹ we disregard this movement and assume that the mass fraction remains at all times at the maximal salt mass fraction of the saturated brine along the fixed boundary, i.e.

$$\omega = \omega_s \text{ at } z = 0, \text{ for all } t \geq 0 \quad (11)$$

Further, the flux of salt entering the flow domain induces a movement of water. This leads to the additional boundary condition, see again Hassanizadeh and Leijnse¹,

$$\left(\mathbf{q} + \frac{D}{(1 - \omega_s)} \text{grad} \omega \right) \cdot \mathbf{n} = 0 \text{ at } z = 0, \text{ for all } t \geq 0 \quad (12)$$

where \mathbf{n} denotes the outward normal at the boundary $\{z = 0\}$. As initial concentration we have $\rho = \rho_f$ or $\omega = 0$

everywhere in the flow region. At large distance above the $\{z = 0\}$ plane we now impose only the y -component of the flow, since the z -component will be determined by the problem. Thus we set

$$q_y \rightarrow q_f \text{ as } z \rightarrow +\infty, \text{ for all } t \geq 0 \quad (13)$$

In both problems the y -coordinate ranges from $-\infty$ to $+\infty$. Therefore, we may look for a density and specific discharge depending only on the z -coordinate and time, i.e.

$$\rho = \rho(z, t) \text{ and } \mathbf{q} = \mathbf{q}(z, t) \quad (14)$$

This assumption implies irrotational flow in both problems. We do not consider perturbations of the initial condition on ρ . Following de Josseling de Jong and van Duijn⁷ we use eqn (14) and Darcy's law (eqn (6)) to obtain a linear algebraic relation between the fluid density and the y -component of the specific discharge. This relation can be found by first taking the curl of eqn (6):

$$\frac{\partial}{\partial z} \left\{ q_y - \frac{\kappa}{\mu} \rho g_y \right\} - \frac{\partial}{\partial y} \left\{ q_z - \frac{\kappa}{\mu} \rho g_z \right\} = 0 \quad (15)$$

and by substituting eqn (14) into this expression. The result is

$$q_y - \frac{\kappa}{\mu} \rho g_y = q_y + \frac{\kappa}{\mu} \rho g \sin \beta = \text{constant in space} \quad (16)$$

where β is the inclination of the $z = 0$ plane. To determine the constant in eqn (16) we use the behavior of q_y and ρ at $z = +\infty$:

$$q_y(\infty, t) = q_f \text{ and } \rho(\infty, t) = \rho_f \text{ for all } t > 0 \quad (17)$$

This yields the relation

$$q_y = q_f - \frac{\kappa}{\mu} (\rho - \rho_f) g \sin \beta \quad (18)$$

Thus in order to determine the pair (ρ, \mathbf{q}) from the differential equations with initial and boundary conditions, there remains by virtue of eqn (18), only to determine ρ and q_z . Using eqn (18), the equations for these quantities reduce to

$$\phi \frac{\partial \rho}{\partial t} + \frac{\partial}{\partial z} (\rho q_z) = 0 \quad (19)$$

and

$$\phi \frac{\partial \rho \omega}{\partial t} + \frac{\partial}{\partial z} \left(\rho \omega q_z - D \rho \frac{\partial \omega}{\partial z} \right) = 0 \quad (20)$$

Combining these equations yields

$$\phi \rho \frac{\partial \omega}{\partial t} + \rho q_z \frac{\partial \omega}{\partial z} = \frac{\partial}{\partial z} \left(\rho D \frac{\partial \omega}{\partial z} \right) \quad (21)$$

and with the equation of state (eqn (7)) we obtain

$$\phi \frac{\partial \rho}{\partial t} + q_z \frac{\partial \rho}{\partial z} = D \frac{\partial^2 \rho}{\partial z^2} \quad (22)$$

We use the coupled system eqns (19) and (22) in our analysis. To determine ρ and q_z from this system we need

to impose the initial and boundary conditions. In Problem I we look for a solution in the domain $\{(z, t): -\infty < z < +\infty, t > 0\}$ subject to the initial condition

$$\rho(z, 0) = \begin{cases} \rho_f & \text{for } z > 0 \\ \rho_s & \text{for } z < 0 \end{cases} \quad (23)$$

and boundary condition eqn (10) for the flow

$$q_z(+\infty, t) = 0 \text{ for all } t \geq 0 \quad (24)$$

We note that a condition on the flow such as eqn (24) is natural for the problem. Combining eqns (19) and (22) gives the ordinary differential equation

$$\rho \frac{\partial q_z}{\partial z} + D \frac{\partial^2 \rho}{\partial z^2} = 0 \quad (25)$$

Thus knowing ρ , a single condition on q_z [e.g. Eqn (24)] is needed to determine the solution. The specific choice is arbitrary. In fact one could construct a solution corresponding to any given $q_z(+\infty, t)$. We also observe at this point that eqn (25), when writing it in the form

$$\text{div } \mathbf{q} = \frac{\partial q_z}{\partial z} = -\frac{1}{\rho} \text{div}(D \text{grad } \rho) \quad (26)$$

clearly demonstrates the coupling between brine transport by diffusion–dispersion, creating a non-zero divergence in the flow field, and hence enhanced fluid flow. Density gradients imply fluid movement and vice versa.

Problem II is solved in the domain $\{(z, t): z > 0, t > 0\}$ where we impose initially

$$\rho(z, 0) = \rho_f \text{ for } z > 0 \quad (27)$$

and along the boundary, see eqns (11) and (12)

$$\rho(0, t) = \rho_{sm} := \rho_f e^{\gamma \omega_s} \quad (28)$$

and

$$q_z(0, t) = -\frac{D}{\gamma \rho_{sm} (1 - \omega_s)} \frac{\partial \rho}{\partial z}(0, t) \quad (29)$$

for all $t > 0$. Here ρ_{sm} denotes the density of saturated brine. Boundary condition (3.3) relates the specific discharge to the spatial derivative of the fluid density at the salt rock boundary. Although no water is being produced along the salt rock boundary, a non-zero discharge exists along that boundary due to volume effects caused by high salt concentration gradients in the fluid. In fact, at the salt rock boundary, the fluid mass flux is balanced by the diffusive–dispersive mass flux. For details on the derivation of this salt rock boundary condition we refer to Hassanizadeh and Leijnse¹. As will be shown in a later section of this paper, the particular form of eqn (29) allows a straight forward similarity transformation.

4 DIMENSIONLESS VARIABLES

Before discussing eqns (19) and (22) we introduce the dimensionless variables

$$\rho^* = \frac{\rho - \rho_f}{\tilde{\rho}_s - \rho_f}, q_z^* = \frac{q_z}{\frac{\kappa}{\mu} \rho_f g}, z^* = \frac{\frac{\kappa}{\mu} \rho_f g}{D} z, t^* = \frac{\left(\frac{\kappa}{\mu} \rho_f g\right)^2}{\phi D} t \tag{30}$$

and

$$\varepsilon = \frac{\tilde{\rho}_s - \rho_f}{\rho_f} \tag{31}$$

where $\tilde{\rho}_s = \rho_s$ in Problem I and $\tilde{\rho}_s = \rho_{sm}$ in Problem II. In terms of these new variables the equations become (dropping the asterisks notation)

$$\frac{\partial \rho}{\partial t} + \frac{\partial}{\partial z}(\rho q_z) + \frac{1}{\varepsilon} \frac{\partial q_z}{\partial z} = 0 \tag{32}$$

and

$$\frac{\partial \rho}{\partial t} + q_z \frac{\partial \rho}{\partial z} = \frac{\partial q_z^2}{\partial z^2} = 0 \tag{33}$$

The rescaled initial and boundary conditions in Problem I are

$$\rho(z, 0) = \begin{cases} 0 & \text{for } z > 0 \\ 1 & \text{for } z < 0 \end{cases} \tag{34}$$

and

$$q_z(+\infty, t) = 0 \text{ for all } t > 0 \tag{35}$$

In Problem II the scaling eqns (30) and (31) lead to

$$\rho(z, 0) = 0 \text{ for } z > 0 \tag{36}$$

$$\rho(0, t) = 1 \text{ for } t > 0 \tag{37}$$

and

$$q_z(0, t) = -\varepsilon K(\varepsilon) \frac{\partial \rho}{\partial z}(0, t) \tag{38}$$

where $K(\varepsilon)$ is given by:

$$K(\varepsilon) = \frac{\rho_f}{\rho_{sm} \gamma (1 - \omega_s)} \frac{1}{(1 + \varepsilon)(\gamma - \log(1 + \varepsilon))} \tag{39}$$

Note that the relative density differences lies in the interval

$$0 < \varepsilon < e^{\gamma \omega_s} - 1 \approx 2^{\omega_s} - 1 \approx 0.2 \tag{40}$$

for $\omega_s = 0.26$

5 SELF-SIMILAR SOLUTIONS

Due to the non-linear coupling between eqns (32) and (33) it is not possible to find explicit, closed-form solutions of Problems I and II. Nevertheless, their special structure enables us to obtain much information concerning the

qualitative behavior of the solutions and to obtain accurate approximations.

The key idea is to look for self-similar solutions, which reduce eqns (32) and (33) to a set of coupled ordinary differential equations with boundary conditions originating from eqns (34)–(38). The transformed problems were studied in detail by van Duijn et al.⁴. They considered fundamental questions related to existence and uniqueness of solutions, as well as their qualitative behavior. With respect to the latter, they showed certain monotonicity properties of solutions and their asymptotic behavior for $|z| \rightarrow \infty$ and for $\varepsilon \downarrow 0$. Some of these results will be discussed here and in Section 7.

The similarity transformations for Problems I and II are given by

$$\eta = \frac{z}{\sqrt{t}} \tag{41}$$

and

$$\rho(z, t) = u(\eta) \text{ and } q_z(z, t) = \frac{1}{\sqrt{t}} v(\eta) \tag{42}$$

This results in the set of differential equations

$$(uv)' + \frac{1}{\varepsilon} v' - \frac{1}{2} \eta u' = 0 \tag{43}$$

$$u'v - \frac{1}{2} \eta u' = u'' \tag{44}$$

where the primes denote differentiation with respect to η . The independent variable η ranges from $-\infty$ to $+\infty$ in Problem I and from 0 to $+\infty$ in Problem II.

The following boundary conditions for $u(\eta)$ and $v(\eta)$ in Problem I result from eqns (34) and (35) and are found to be

$$u(-\infty) = 1 \text{ and } u(+\infty) = 0 \tag{45}$$

and

$$v(+\infty) = 0 \tag{46}$$

For Problem II we find from eqns (36)–(38)

$$u(0) = 1 \text{ and } u(+\infty) = 0 \tag{47}$$

and

$$v(0) = -K(\varepsilon) \varepsilon u'(0) \tag{48}$$

Eqns (43) and (44) can be combined into:

$$u'' + \left(\frac{1}{2} \eta - v\right) u' = 0 \tag{49}$$

$$v' = -\frac{u''}{u + \frac{1}{\varepsilon}} \tag{50}$$

Let us first discuss Problem I. We start with the important observation that solutions (u, v) of equations eqns (49) and (50) on \mathbf{R} are invariant under linear shifts. By this we mean the following. For any given $a \in \mathbf{R}$, let

$$\bar{\eta} = \eta - a, \bar{u}(\bar{\eta}) = u(\eta) \text{ and } \bar{v}(\bar{\eta}) = v(\eta) - \frac{1}{2} a \tag{51}$$

Then if $[u(\eta), v(\eta)]$ solves eqns (49) and (50) for $-\infty < \eta < +\infty$, then so does $[\bar{u}(\bar{\eta}), \bar{v}(\bar{\eta})]$ if we replace η by $\bar{\eta}$ in eqn

(49). This means that if $[u(\eta), v(\eta)]$ is a solution for which $v(\pm \infty)$ exists, then by shifting η over a suitable distance a , we can reach any limiting value of $v(\eta)$, either at $\eta = -\infty$ or at $\eta = +\infty$. If we choose $a = 2v(+\infty)$ in eqn (51) we can ensure that eqn (46) is satisfied. This invariance property will be used in both the mathematical and numerical procedures for solving Problem I.

Before discussing the construction of solutions, we recall some a priori properties which give an idea about the qualitative behavior of the solution. We proved in Van Duijn et al.⁴ that

1. $u'(\eta) < 0$ for all $-\infty < \eta < +\infty$;
2. there exists $\eta_0 > 0$ such that $u''(\eta) < 0$ for $\eta < \eta_0$ and $u''(\eta) > 0$ for $\eta > \eta_0$
3. $v(\eta_0) = \frac{1}{2}\eta_0$ and $v'(\eta) > 0$ for $\eta < \eta_0$ and $v'(\eta) < 0$ for $\eta > \eta_0$
4. $u'(\eta) \rightarrow 0$ if $|\eta| \rightarrow \infty$

The first assertion implies that the brine concentration increases strictly with depth and is concave below the plane $z = \eta_0\sqrt{t}$ and convex above it. Also the z -component of the specific discharge has a maximum at $z = \eta_0\sqrt{t}$ of magnitude $q_z(\eta_0sqtt, t) = \frac{1}{2}\eta_0/\sqrt{t}$. The number η_0 plays a prominent role in simultaneous transport of brine and radionuclides, which will be explained in Section 8.

Next we turn to the solution procedure. As a first observation we note that eqns (49)–(51) can be combined into a single equation with η missing. This equation, having the form

$$\frac{1}{2} + \left(\frac{u''}{u'}\right)' = -\frac{u''}{u + \frac{1}{\varepsilon}} \text{ with } -\infty < \eta < +\infty \tag{52}$$

needs three conditions to be solved uniquely. Two conditions are given by eqn (45). As a third condition we take, for instance,

$$u(0) = \frac{1}{2} \tag{53}$$

We outline below how to obtain a unique solution satisfying eqns (52), (45) and (53) and how to obtain from that solution a corresponding $v = v(\eta)$ so that the pair (u, v) satisfies eqns (43) and (44). This function v will not satisfy eqn (46). To achieve that condition one applies the linear shift (eqn (51)) with $a = 2v(\infty)$.

Eqn (52) is of third order, non-linear and defined on an unbounded domain. To tackle it directly is, therefore, not straightforward. As so often in mathematics, we solve problems by combining and applying what we already know. Also in this case, we will transform eqn (52) into a second order equation on a finite domain, yielding a boundary value problem which is well known in the mathematical literature. This transformation is achieved by taking u as the independent variable, which is allowed

by the monotonicity of u , and by taking u' as the new independent variable. Thus setting

$$\eta = \eta(u) \text{ and } y(u) = -u'(\eta(u)) \tag{54}$$

we obtain

$$y\{(1 + \varepsilon u)y'\}' = -\frac{1}{2}(1 + \varepsilon u), \quad 0 < u < 1 \tag{55}$$

In view of property (4) we obtain for y the boundary conditions

$$y(0) = 0 \text{ and } y(1) = 0 \tag{56}$$

By setting further

$$s = \frac{\log(1 + \varepsilon u)}{\log(1 + \varepsilon)} \text{ and } z(s) = \frac{\varepsilon}{\log(1 + \varepsilon)}y(u) \tag{57}$$

we obtain the problem

$$(I') \begin{cases} -zz'' = \frac{1}{2}e^{2s\log(1 + \varepsilon)}, & z > 0 \text{ for } 0 < s < 1 \\ z(0) = z(1) = 0 \end{cases} \tag{58}$$

which is well known and arises in the study of self-similar solutions of non-linear diffusion equations, see for instance Esteban et al.¹⁵, Van Duijn and Peletier¹⁶, Van Duijn and Floris¹⁷ and Van Duijn et al.¹⁸. In the context of nonlinear diffusion one calls eqn (58) the flux equation, because it specifies the flux in terms of the concentration. One sees immediately (since $z > 0$) that

$$z''(s) < 0 \text{ for } 0 < s < 1 \tag{59}$$

Less straightforward are the proofs of the properties

$$\lim_{s \downarrow 0} z'(s) = +\infty \text{ and } \lim_{s \uparrow 1} z'(s) = -\infty \tag{60}$$

which can be found in Van Duijn and Floris¹⁷. Knowing that a solution $z = z(s)$ of Problem I' exists and is unique, and knowing much about its qualitative behavior, one finds $y = y(u)$ from eqn (57). Finally, the solution $u = u(\eta)$ satisfying eqns (52), (45) and (53) is implicitly defined by

$$\eta(u) = \int_u^{\frac{1}{2}} \frac{1}{y(s)} ds \tag{61}$$

which results from integrating eqn (54). The corresponding $v = v(\eta)$ is given by

$$v(\eta) = \frac{1}{2}\eta - y'(u(\eta)) \text{ for } -\infty < \eta < +\infty \tag{62}$$

which follows from eqns (49) and (54).

Since Problem II is defined on the semi-infinite interval $0 < \eta < +\infty$, we loose invariance property eqn (51). But the other properties (1)...(4) remain the same, when taking $0 < \eta < +\infty$, yielding a similar qualitative

picture of the solution. The solution procedure proceeds along the same lines. It leads to the transformed problem

$$(II') \begin{cases} -zz'' = \frac{1}{2}e^{2s \log(1+\varepsilon)}, & z > 0 \text{ for } 0 < s < 1 \\ z(0) = 0, \quad z'(1) = -Lz(1) \end{cases} \quad (63)$$

where L is a constant given by

$$L = K(\varepsilon)(1 + \varepsilon)\log(1 + \varepsilon) = \frac{\log(1 + \varepsilon)}{\gamma - \log(1 + \varepsilon)} \quad (64)$$

The boundary condition at $s = 1$ is a direct consequence of eqn (48). To return to $u = u(\eta)$, we first use again eqn (57) to obtain $y = y(u)$ and then

$$\eta \int_{u(\eta)}^1 \frac{1}{y(s)} ds \text{ for } 0 < \eta < +\infty \quad (65)$$

The corresponding $v = v(\eta)$ is obtained from eqn (62).

6 NUMERICAL PROCEDURES AND RESULTS

The mathematical analysis has provided us with qualitative information about the structure of the solutions of Problem I and II. This information can be used to develop procedures to obtain accurate numerical solutions.

Starting point for both problems is the third order eqn (52). We write this equation as a system of first order equations by setting

$$p = u, \quad q = u' \text{ and } r = v \quad (66)$$

Substitution in eqn (52) yields

$$(S) \begin{cases} p' = q \\ q' = q \left(r - \frac{1}{2}\eta \right) \\ r' = -\frac{q \left(r - \frac{1}{2}\eta \right)}{p + \frac{1}{\varepsilon}} \end{cases} \quad (67)$$

To solve this system we impose three conditions at $\eta = 0$:

$$p(0) = u(0) = p_0, \quad q(0) = u'(0) = q_0, \quad r(0) = v(0) = r_0 \quad (68)$$

where $p_0 = 1/2$ (Problem I) or $p_0 = 1$ (Problem II), and where q_0 and r_0 are a priori unknown. They have to be determined from the boundary conditions eqn (45) (Problem I) or from eqns (47) and (48) (Problem II).

Concerning Problem I, one approach is to apply a shooting procedure in the regions $\{\eta < 0\}$ and $\{\eta > 0\}$. Taking for (S) the initial values $p_0 = 1/2$ and q_0, r_0 arbitrary, one solves the equations for $\{\eta < 0\}$ and $\{\eta > 0\}$. The idea is to choose p_0 and q_0 such that

$$p(-\infty) = u(-\infty) = 1 \text{ and } p(+\infty) = u(+\infty) = 0 \quad (69)$$

However, this procedure is not at all trivial because there

are two degrees of freedom in the problem. Moreover, it would be time consuming to compute accurate values for q_0 and r_0 by trial and error such that the correct limiting behavior for u at $\eta = + / - \infty$ is achieved.

An alternative approach is to determine q_0 and r_0 directly from Problem (I') by noting that

$$p_0 = -y\left(\frac{1}{2}\right) = \frac{\log(1 + \varepsilon)}{\varepsilon} z\left(\frac{\log\left(1 + \frac{\varepsilon}{2}\right)}{\log(1 + \varepsilon)}\right) \quad (70)$$

and, using eqn (48),

$$r_0 = -y'\left(\frac{1}{2}\right) = \frac{1}{1 + \frac{\varepsilon}{2}} z'\left(\frac{\log\left(1 + \frac{\varepsilon}{2}\right)}{\log(1 + \varepsilon)}\right) \quad (71)$$

We find approximate values of the shooting parameters q_0 and r_0 by solving (I') numerically. We omit the details of the computations. Next equations (S) are solved using a fourth order Runge-Kutta method in the regions $\{\eta < 0\}$ and $\{\eta > 0\}$, subject to p_0, q_0 and r_0 . This gives the solution $[u(\eta), v(\eta)]$ of eqns (49) and (50) which satisfies $u(0) = 1/2$. It also provides us with the value of $v(+\infty) = r(+\infty)$ which we need to obtain the correct shift $a = 2v(+\infty)$ to satisfy boundary condition eqn (46).

In all cases considered, i.e. for all relevant values of ε , we verified the boundary conditions $u(+\infty) = 0$ and $u(-\infty) = 1$. Up to a small error term ($\approx \pm 10^{-6}$) these values are reproduced by the numerical approximations. This serves as an independent check for the accuracy of the numerical procedure for Problem (I').

Figs 2 and 3 give the results of the numerical approximations of the similarity solutions $u(\eta)$ and $v(\eta)$ for different values of the relative density difference ε .

The value $\varepsilon = 0.025$ corresponds to sea water. This curve is not distinguishable from the curve for $\varepsilon = 0$ on the scale of Fig. 2. The limit $\varepsilon \rightarrow 0$ is the so-called Boussinesq approximation of Boussinesq limit, see Section 7. The value $\varepsilon = 0.2$ corresponds with an almost saturated brine, while $\varepsilon = 0.5$ (although physically not possible) is chosen here to emphasize the effect. Observe that the numerical solutions satisfy the qualitative behavior discussed in Section 5.

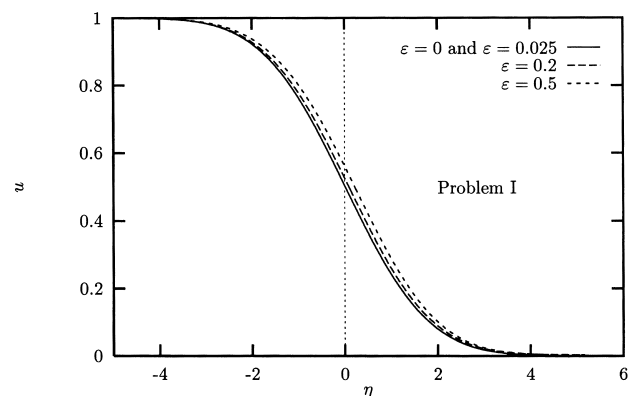


Fig. 2. Numerical approximations of $u(\eta)$ for Problem I.

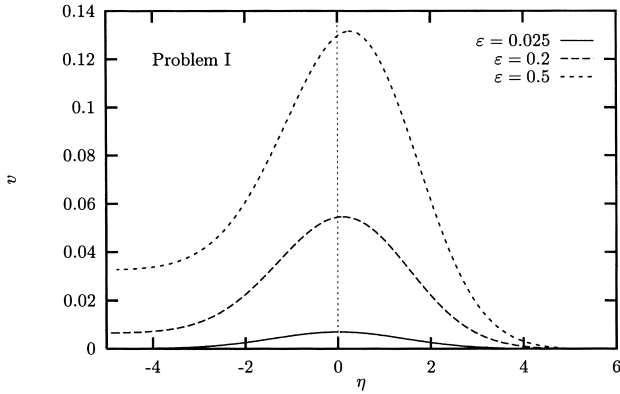


Fig. 3. Numerical approximations of $v(\eta)$ for Problem I.

Concerning Problem II we solve system (S) for $\eta > 0$ subject to the initial conditions

$$p(0) = u(0) = 1 \tag{72}$$

$$q(0) = u'(0) = q_0 < 0$$

$$r(0) = v(0) = -\varepsilon K(\varepsilon)q_0$$

where the last condition is a consequence of eqn (48). This is a one-parameter shooting problem which is more straightforward and is solved without using Problem (II'). The object is to find an approximate value of q_0 such that the boundary condition $u(+\infty)$ is satisfied. This can be achieved by starting the shooting procedure with an initial estimate for q_0 and check if the corresponding limiting behavior is satisfied at sufficiently large distance L from the origin. The problem is to determine an approximate value of q_0 such that the boundary condition $u(+\infty) = 0$ is satisfied. This can be achieved by starting the shooting procedure with an estimated value of q_0 and check if the corresponding limiting behavior is satisfied at a sufficiently large distance L from the origin. If $u(L) > \delta > 0$, where δ is an a priori specified small error term, the estimated value of q_0 is decreased by a fixed amount Δq_0 and the shooting procedure is repeated. The step size Δq_0 remains fixed until, say after the n th step, $u^n(L) < 0$. Now q_0^n is increased by the bisection of Δq_0 , hence $q_0^{(n+1)} = q_0^0 - \Delta q_0(n - (1/2))$. If $u^{n+1}(L) > \delta$ or if $u^{n+1}(L) < 0$ we bisect the last alteration

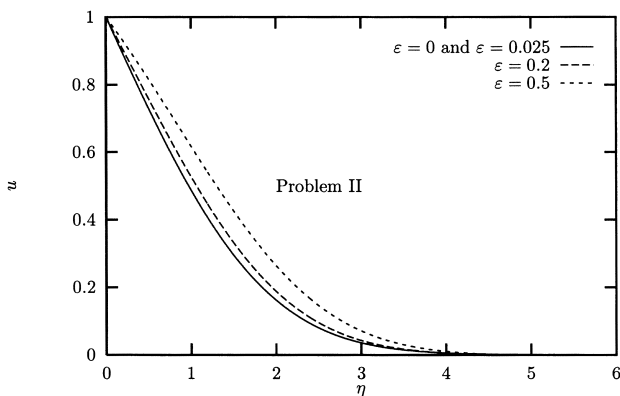


Fig. 4. Numerical approximations of $u(\eta)$ for Problem II.

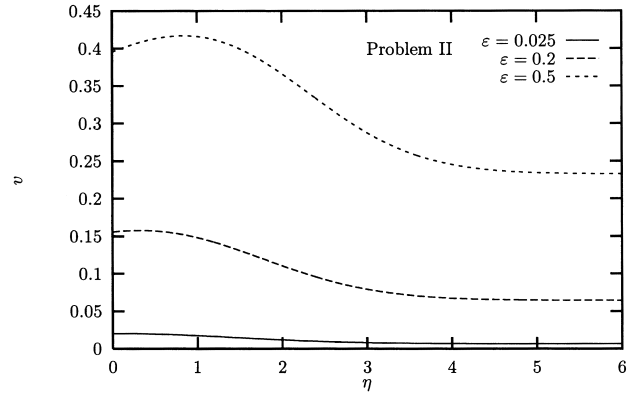


Fig. 5. Numerical approximations of $v(\eta)$ for Problem II.

of q_0 again and obtain, respectively: $q_0^{n+2} = q_0^0 - \Delta q_0(n - (1/4))$ or $q_0^{n+2} = q_0^0 - \Delta q_0(n - (3/4))$. This procedure is repeated until $0 \leq u(L) \leq \delta$. The number of steps depends on the quality of the initial guess of q_0 and the initial step size Δq_0 .

Fig. 4 shows the results of the iterative shooting procedure for the scale density $u(\eta)$ for different ε -values. The corresponding scaled specific discharge distributions $v(\eta)$ are given in Fig. 5. Notice that $v(0) \neq 0$. This is a consequence of boundary condition eqn (48) at the salt rock–brine interface. Because u is a decreasing function we have $u'(0) < 0$, hence $v(0) > 0$, for all $\varepsilon > 0$.

Figs 6 and 7 give the relative density $\rho(z, t) = u(z/\sqrt{t})$ and the unscaled specific discharge $q_z(z, t) = v(z/\sqrt{t})/\sqrt{t}$ at different time levels in the original variables. The other parameter values used in these examples are adopted from Herbert et al.¹⁰ and listed in Table 1.

Remark (boundary condition): If we impose, instead of eqn (48), the condition $q_z(0, t) = 0$ for all $t > 0$ to express the assumption that the salt rock boundary is impervious, then the analysis yields $v(\eta) < v(0) = 0$ for all $\eta > 0$. An explanation for this behavior is that $q_z = 0$ at the boundary can only be maintained by a back flow coming from $+\infty$. We conclude that this is a physically unrealistic situation and that the no flow boundary is incompatible with the model discussed in this paper.

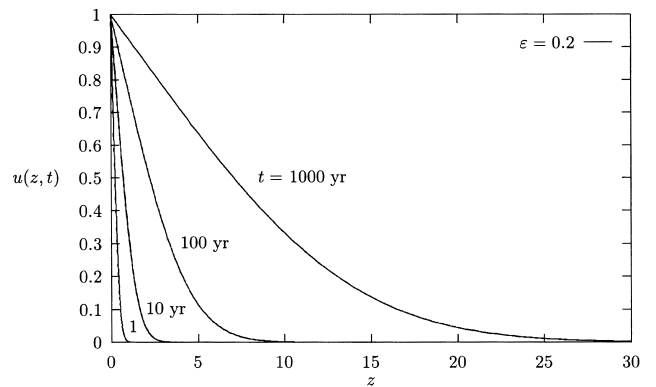


Fig. 6. Brine density profiles at different times for $\varepsilon = 0.2$ in Problem II.

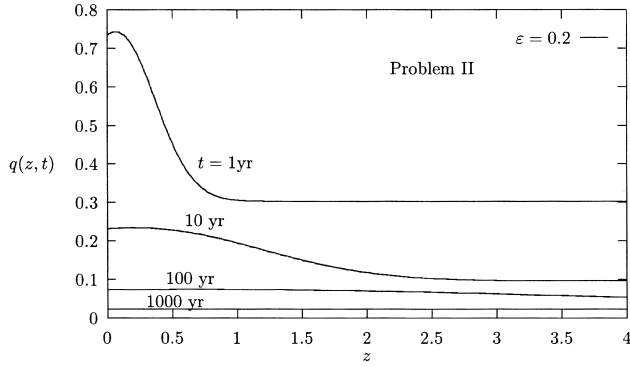


Fig. 7. Specific discharge at different times for $\varepsilon = 0.2$ in Problem II.

Table 1.

Property	Value	Physical unit
κ	10^{-12}	m^2
μ	10^{-3}	Pas
g	9.81	m s^{-2}
ϕ	0.3	—
ρ_f	1000	kg m^{-3}
D	10^{-9}	$\text{m}^2 \text{s}^{-1}$

Some results of a formal asymptotic analysis are given in the Appendix A of this paper. This analysis yields series expansions in terms of the relative density difference ε for the similarity solutions $u(\eta)$ and $v(\eta)$. When these expansions are truncated we obtained approximation formulas, up to a certain (known) accuracy.

7 TRANSPORT OF RADIONUCLIDES

In this section we consider the simultaneous transport of a non-adsorbing radionuclide, occurring in tracer concentrations, in the vicinity of a salt dome. We assume that the flow geometry is given by Problem II, resulting in one-dimensional (z -direction) transport. The equation to be solved is

$$R\phi \frac{\partial \rho \omega_c}{\partial t} + \frac{\partial}{\partial z} \left(\rho \omega_c q_z - D_c \rho \frac{\partial \omega_c}{\partial z} \right) - \phi \lambda \rho \omega_c = 0 \quad (73)$$

where ω_c denotes the mass fraction of a radionuclide, λ the decay constant, R the retardation factor for linear equilibrium adsorption, and D_c its effective diffusivity–dispersivity. Note that $q_z = q_z(z, t)$ and $\rho = \rho(z, t)$ are solutions of Problem II. Further, note that in general $D_c \neq D$, the diffusivity of the salt. We introduce the parameter θ , defined as

$$\theta = D_c/D \quad (74)$$

and apply the scaling rules eqn (30) in eqn (73). This ensures identical time scales for brine and radionuclide transport. The radionuclide mass fraction is scaled according to

$$\omega_c^* = \frac{\omega_c}{\omega_0} \quad (75)$$

where ω_0 denotes a reference mass fraction, e.g. the

(radionuclide) mass fraction at the salt rock boundary. As a consequence of eqn (30) we find

$$\lambda^* = \frac{R\phi D}{\left(\frac{\kappa}{\mu} \rho_f g \right)^2} \lambda \quad (76)$$

as the dimensionless decay constant. Combining eqns (73) and (19), and applying eqns (30), (74)–(76), we obtain (omitting the asterisks)

$$\frac{\partial \bar{\omega}_c}{\partial t} + q_z \frac{\partial \bar{\omega}_c}{\partial z} - \frac{\theta}{(\varepsilon \rho + 1)} \frac{\partial}{\partial z} \left((\varepsilon \rho + 1) \frac{\partial \bar{\omega}_c}{\partial z} \right) = 0 \quad (77)$$

in which we eliminated the decay term in the usual way, i.e. by setting $\omega_c(z, t) = \bar{\omega}_c(z, t)e^{-\lambda^* t}$. The boundary and initial conditions are

$$\bar{\omega}_c(0, t) = 1 \text{ for all } t > 0 \quad (78)$$

$$\bar{\omega}_c(z, 0) = 1 \text{ for all } z > 0$$

Since $q_z(z, t) = v(\eta)/\sqrt{t}$ and $\rho(z, t) = u(\eta)$, we note that eqns (77) and (78) have a self similar solution $\bar{\omega}_c(z, t) = f(\eta)$, where f is a solution of the linear boundary value problem

$$(BVP) \begin{cases} f'(v - \frac{\eta}{2}) - \frac{\theta}{(\varepsilon u + 1)} ((\varepsilon u + 1)f')' = 0 \\ f(0) = 1 \\ f(\infty) = 0 \end{cases} \quad (79)$$

To solve this problem we first eliminate v using eqn (49) and next integrate the resulting equation. This leads to

$$\begin{aligned} f(\eta) &= 1 - \frac{\int_0^\eta \left(\frac{u'(\xi)}{u'(0)} \right)^{\frac{1}{\theta}} \frac{(1+\varepsilon)}{\varepsilon u(\xi) + 1} d\xi}{\int_0^\infty \left(\frac{u'(\xi)}{u'(0)} \right)^{\frac{1}{\theta}} \frac{(1+\varepsilon)}{\varepsilon u(\xi) + 1} d\xi} \\ &= 1 - \frac{\int_0^\eta \frac{|u'(\xi)|^{\frac{1}{\theta}}}{\varepsilon u(\xi) + 1} d\xi}{\int_0^\infty \frac{|u'(\xi)|^{\frac{1}{\theta}}}{\varepsilon u(\xi) + 1} d\xi} \end{aligned} \quad (80)$$

where u is the solution of Problem II, for a given value of ε . The corresponding, scaled radionuclide concentration is

$$\bar{c}(\eta) = f(\eta) \frac{\varepsilon u(\eta) + 1}{\varepsilon + 1} \quad (81)$$

For $\theta = 1$ we can evaluate eqn (80) and obtain

$$\bar{c}(\eta) = \frac{\varepsilon u(\eta) + 1}{\varepsilon + 1} \left(1 - \frac{\log \left(\frac{\varepsilon u(\eta) + 1}{\varepsilon + 1} \right)}{\log \left(\frac{1}{\varepsilon + 1} \right)} \right) \quad (82)$$

Fig. 8 shows the scaled concentration \bar{c} for different values of θ and $\varepsilon = 0.2$. The results in this figure indicate that, as θ

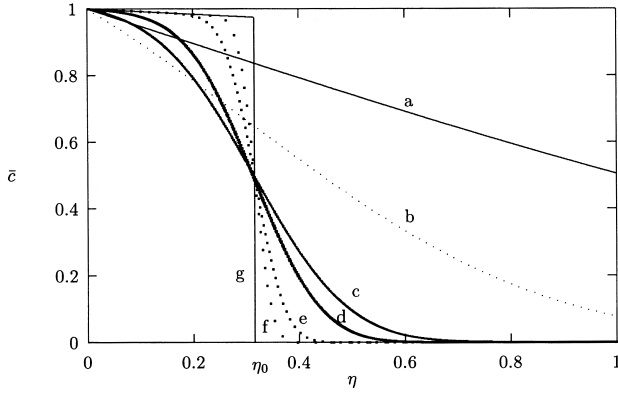


Fig. 8. The scaled radionuclide concentration $\bar{c}(\eta)$ for $\varepsilon = 0.2$ and different values of θ : (a), $\theta = 1.0$; (b), $\theta = 0.1$; (c), $\theta = 0.01$; (d), $\theta = 0.005$; (e), $\theta = 0.001$; (f), $\theta = 0.0003$; and (g), $\theta = 0.0$.

$\rightarrow 0$, the concentration \bar{c} has a discontinuity at $\eta = \eta_0 \approx 0.316$ with $\bar{c} = 0$ for $\eta > \eta_0$. This is a direct consequence of the limiting behavior of (BVP) as $\theta \rightarrow 0$: i.e.

$$\begin{cases} f'(v - \frac{\eta}{2}) = 0 & \text{for all } \eta > 0 \\ f(0) = 1, f(\infty) = 0 \end{cases} \quad (83)$$

which implies a piecewise constant solution

$$f(\eta) = \begin{cases} 1 & \text{for } 0 < \eta < \eta_0 \\ 0 & \text{for } \eta > \eta_0 \end{cases} \quad (84)$$

and thus

$$\bar{c}(\eta) = \begin{cases} \frac{\varepsilon u(\eta) + 1}{\varepsilon + 1} & \text{for } 0 < \eta < \eta_0 \\ 0 & \text{for } \eta > \eta_0 \end{cases} \quad (85)$$

As a consequence, a radionuclide front emerges which moves with speed $v(\eta_0/\sqrt{t})$, where $v(\eta) = \max((v(\eta)) = \eta_0/2$, see property (3) in Section 5. The position of the front in the (z, t) -plane is given by $s(t) = 2v(\eta_0)\sqrt{t} = \eta_0\sqrt{t}$, which is equivalent to the path of a tracer particle released at $t = 0$ in $z = 0$, i.e. at the beginning of the brine transport process. Hence in the limit $\theta \rightarrow 0$, the movement of the tracer is caused by the compressibility effect only.

8 DISCUSSION

Self-similar solutions make the analysis tractable and (semi-) explicit results can be obtained. A crucial requirement for the applicability of similarity arguments is that both the governing equations and initial and/or boundary conditions be reducible to the similarity form. Hence, only in special cases one may expect to find similarity solutions. Due to the piecewise initial density distribution in Problem I and II we may consider the obtained similarity solutions as upper limits for the compressibility effect. Smooth initial data decrease the magnitude of the enhanced flow.

In analyzing Problems I and II we show explicitly the effect of enhanced groundwater flow due to compressibility of fluid caused by high salt concentration gradients. Characteristic for both problems is the occurrence of additional specific discharge in a direction perpendicular to the main groundwater direction. In both problems q_z is not influenced by gravity. The only quantity that depends on gravity is the specific discharge in the y -direction, parallel to main flow q_f .

The flow geometry of both problems and the boundary-initial conditions are chosen such that semi-analytical solutions are obtained. These solutions allow us to study the relative importance of volume effects in terms of the relative density difference. Although the flow of groundwater in the vicinity of a 'real' salt dome is more complex, the simplified problems studied in this paper gain insight in the non-linear coupling between fluid density and fluid flow due to volume effects.

The salt rock boundary condition, which relates the fluid mass flux to the diffusive-dispersive mass flux at the salt boundary, is physically more realistic than the often used no-flow condition $q_z(0, t) = 0$. The latter induces a back flow coming from $z = +\infty$ to maintain the no-flow condition at $z = 0$, see the remark in Section 6.

In this paper we only consider constant (molecular) diffusion. In a more realistic description a velocity dependent dispersion matrix has to be introduced into eqn (5). Molecular diffusion underestimates the compressibility effects.

When transversal dispersion, due to the (regional) back ground flow q_y , dominates the dispersion-diffusion in the z -direction we arrive at a different situation. Under the assumption $|q_z| < |q_y|$ eqn (8) reduces to

$$D \approx \phi D_{\text{mol}} + \alpha_T |q_y| = \quad (86)$$

$$\phi D_{\text{mol}} + \alpha_T |q_f - \frac{\kappa}{\mu} (\rho - \rho_f) g \sin \beta| \quad (87)$$

yielding D as a function of ρ . The analysis of this case is quite different from what we discussed here and will be published elsewhere¹⁸.

If $q_f \gg \frac{\kappa}{\mu} (\rho_s - \rho_f) g \sin \beta$ we may replace eqn (87) by

$$D \approx \phi D_{\text{mol}} + \alpha_T |q_f| = \quad (88)$$

yielding a constant dispersivity which is in general much larger than the effective molecular diffusivity ϕD_{mol} . The number

$$P = \frac{\alpha_T |q_f|}{\phi D_{\text{mol}}} \quad (89)$$

indicates the relative importance of (transversal) dispersion with respect to molecular diffusion. If $P < 1$ diffusion dominates dispersion. When $q_f = 100 \text{ m year}^{-1}$ typical values of the dispersivity are: $D(\alpha_T = 0.1 \text{ m}) \approx 3 \cdot 10^{-7} \text{ m}^2 \text{ s}^{-1}$ and $D(\alpha_T = 1.0 \text{ m}) \approx 3 \cdot 10^{-6} \text{ m}^2 \text{ s}^{-1}$. The corresponding P -numbers are: $\approx 10^3$ and $\approx 10^4$. It is obvious that such values of the dispersivity will enhance the compressibility effects in brine transport.

If we consider longitudinal dispersion of radionuclides in the z -direction eqn (8) reduces to

$$D(q_z) = D_c + \alpha_L |q_z| \quad (90)$$

remembering that $D_c = \phi D_{c-mol} = \theta D$. By virtue of the $1/\sqrt{t}$ -decay of $q_z(z, t)$ one expects the longitudinal dispersion to dominate diffusion only on the short time scale in Problem II. A rough estimate of the order to magnitude of the time \hat{t} after which diffusion becomes dominant can be given by using the approximation $q_z(z, t) \approx v_\varepsilon(0)/\sqrt{t}$ in

$$P = \frac{\alpha_L |q_z(z, t)|}{D_c} < 1 \quad (91)$$

hence

$$\hat{t} \approx \left(\frac{\alpha_L \varepsilon}{\gamma} \right)^2 \frac{\phi}{\pi \theta D} \quad (92)$$

For the case $\theta = D_c/D = 1$, typical values of \hat{t} are: $\hat{t}(\alpha_L = 1 \text{ m}) \approx 0.9$ year and $\hat{t}(\alpha_L = 10 \text{ m}) \approx 88$ year, whereas the typical time scale of brine transport processes is usually in the order of thousands of years. Hence at a very early stage of the brine transport process molecular diffusion starts to dominate longitudinal dispersion. Notice that \hat{t} decreases when we replace the effective molecular diffusivity by a constant transversal diffusivity $\alpha_T q_f$, as discussed above.

9 CONCLUSIONS

1. Compressibility effects in brine transport in porous media are small and have in most practical cases only little effect on the density distributions. We studied two specific brine problems and compared the solutions for $\varepsilon > 0$ with the corresponding Boussinesq solutions for $\varepsilon \rightarrow 0$, where σ denotes the relative density difference.
2. We found that high salt concentration gradients induce a convective flux, which is perpendicular to the main groundwater flow direction in the problems studied in this paper. The magnitude of this flux depends upon the relative density difference and the effective diffusivity–dispersivity of salt.
3. Taking only molecular diffusion into account underestimates the convective brine transport perpendicular to the main flow direction. For the problems studied in this paper it is more realistic to replace the molecular diffusivity by the transversal dispersivity due to the (regional) background flow. This increases the magnitude of q_z significantly and q_z can no longer be neglected as convective transport mechanism.
4. The similarity solutions presented are both of practical and theoretical use. First they provide us with detailed qualitative and quantitative information

about the nature of compressibility effects. Secondly the solutions can be used to verify the accuracy of numerical codes designed to simulate brine transport.

5. The similarity solutions have the following properties: (i) $u'(\eta) < 0$ for all $-\infty < \eta < +\infty$ (Problem I) and $0 \leq \eta < +\infty$ (Problem II); (ii) there exists a number of η_0 such that $u''(\eta) < 0$ for $\eta < \eta_0$ and $u''(\eta) > 0$ for $\eta > \eta_0$; (iii) $v(\eta_0) = \eta_0/2$ and $v'(\eta) < 0$ for $\eta > \eta_0$. The number η_0 plays a prominent role in the simultaneous transport of radionuclides.
6. The results of the asymptotic analysis can be used to approximate the similarity solutions up to a given accuracy.
7. When considering simultaneous transport of brine and dissolved radionuclides we can construct an explicit solution for the radionuclide mass fraction expressed in terms of the solution of the underlying brine problem.
8. In the limit of vanishing radionuclide diffusion–dispersion a radionuclide front emerges in Problem II which travels with speed $v(\eta_0)/\sqrt{t}$. Hence, the movement of the radionuclide is caused by the compressibility effect only.

ACKNOWLEDGEMENTS

We acknowledge S. M. Hassanizadeh (Delft University of Technology, Faculty of Civil Engineering) and T. Leijnse (National Institute of Public Health and Environment Protection (RIVM) in Bilthoven), for bringing this subject to our attention.

REFERENCES

1. Hassanizadeh, S. M. and Leijnse, T. On the modelling of brine transport in porous media. *Water Resources Res.*, 1988, **24**, 321–330.
2. Hassanizadeh, S. M., Experimental study of coupled flow and mass transport: a model validation exercise, Model CARE 90: Calibration in Groundwater Modelling (Proceedings of the conference held in The Hague, September 1990, LAHS Publ. no. 195, 1990.
3. Hassanizadeh, S. M. and Leijnse, T., A non-linear theory of high-concentration-gradient dispersion in porous media, *Adv. Water Res. Research* 1995, (in press).
4. van Duijn, C. J., Peletier, L. A. and Schooting, R. J. On the analysis of brine transport in porous media. *Europ. J. Appl. Math.*, 1973, **4**, 271–302.
5. Glasbergen, O. Extreme salt concentrations in deep aquifers in The Netherlands. *Sci. Total Environ.*, 1988, **24**, 321–330.
6. Roxburgh, I. S., *Geology of High-level Nuclear Waste Disposal — An Introduction*, Chapman and Hall, London, 1987.
7. de Josseling de Jong, G. and van Duijn, C. J. Transverse dispersion from an originally sharp fresh-salt interface caused by shear flow. *J. Hydrol.*, 1986, **84**, 147–163.

8. Oldenburg, C. M. and Pruess, K. Dispersive transport dynamics in a strongly coupled groundwater-brine flow system. *Water Resources Res.*, 1995, **31**(2), 289–302.
9. Carey, A. E., Wheatcraft, S. W., Glass, R. J. and O'Rourke, J. P. Non-fickian ionic diffusion across high concentration gradients. *Water Resources Res.*, 1995, **31**(9), 2213–2218.
10. Herbert, A. W., Jackson, C. P. and Lever, D. A. Coupled groundwater flow and solute transport with fluid density strongly dependent upon concentration. *Water Res. Research*, 1988, **24**, 1781–1795.
11. Swedish Nuclear Inspectorate HYDROCOIN, An international project for studying groundwater hydrology modeling strategies, Level 1 Final Report: Verification of groundwater flow models, Case 5, Swedish Nucl. Insp., Stockholm, 1986.
12. Weast, R. C., *Handbook of Chemistry and Physics*, 63rd ed., CRC Press, Boca Raton, FL, 1982, p. D261.
13. Bear, J., *Dynamics of Fluids in Porous Media*, Elsevier, New York, 1972.
14. Borneman, O. and Fischbeck, R. Ablauung und Hutgesteinsbildung am Salzstock Gorleben. *Z. Geol. Ges.*, 1986, **137**, 71–83.
15. Esteban, J. R., Rodriquez, A. and Vazquez, J. L. A non-linear heat equation with singular diffusivity. *Comm. Part. Diff. Eq.*, 1988, **13**(8), 985–1039.
16. van Duijn, C. J. and Peletier, L. A. A class of similarity solutions of non-linear diffusion equations. *Arch. Rational Mech. Anal.*, 1977, **65**, 363–377.
17. van Duijn, C. J. and Floris, F. J. T., Mathematical analysis of the influence of power law fluid rheology on a capillary diffusion zone, *J. of Petr. Sci. Engng* 1992 (in press).
18. van Duijn, C. J., Gomez, S. M. and Zhang, Hongfei On a class of similarity solutions of the equation $u_t = (|u|^{m-1}u_x)_x$ with $m > -1$. *IMA J. Appl. Math.*, 1988, **41**, 147–163.
19. Maple, Verson Maple V. Release 3, Computer algebra package (software), Waterloo Maple Software, Canada, 1994.

APPENDIX A APPROXIMATE SELF SIMILAR SOLUTIONS

In this Appendix we give some results of a formal asymptotic analysis which can be found in detail in van Duijn et al.⁴. The asymptotic analysis yields series expansions in terms of the relative density difference ϵ for the similarity solutions $[u(\eta), v(\eta)]$ in both problems. When these expansions are truncated we obtain approximation formulas which can be of practical use to approximate $[u(\eta), v(\eta)]$ up to a certain, known accuracy. To emphasize the dependence on ϵ , we denote the solutions by $[u_\epsilon(\eta), v_\epsilon(\eta)]$. In the limit $\epsilon \rightarrow 0$ the solutions (u_ϵ, v_ϵ) converge to the corresponding Boussinesq limit (u_0, v_0) for both problems. For Problem I $v_0 = 0$, while the limit for u_0 is the solution of

$$B_I \begin{cases} u_0'' + \frac{1}{2}\eta u_0' = 0 \text{ for } -\infty < \eta < +\infty \\ u_0(-\infty) = 1 \text{ and } u_0(+\infty) = 0 \end{cases} \quad (A1)$$

and is given by

$$u_0(\eta) = \frac{1}{2} \operatorname{erfc}\left(\frac{\eta}{2}\right) \quad (A2)$$

If we integrate eqn (50) over $(\eta, +\infty)$ and apply the boundary condition $v(+\infty) = 0$ we obtain

$$v(\eta) = -\epsilon \frac{u'(\eta)}{(1 + \epsilon u(\eta))} + \epsilon^2 \int_{\eta}^{+\infty} \frac{(u'(s))^2}{(1 + \epsilon u(s))^2} ds \quad (A3)$$

By eqn (A3) we have

$$\lim_{\epsilon \rightarrow 0} \frac{v(\eta)}{\epsilon} = -u_0'(\eta) \quad (A4)$$

The expression can be used as a first order approximation of $v_\epsilon(\eta)$. We can improve the quality of the approximation by adding more terms in the expansion

$$v_\epsilon(\eta) = -u_0(\eta)\epsilon + \{E_1(\eta) + o(1)\}\epsilon^2 \quad (A5)$$

where

$$E_1(\eta) = 2u_0(\eta)u_0'(\eta) - \frac{1}{2}u_0''(\eta) + \int_{\eta}^{\infty} \{u_0'(s)\}^2 ds \quad (A6)$$

The symbol $o(1)^\dagger$ denotes the order symbol. A similar series expansion for $u_\epsilon(\eta)$ can be derived

$$u_\epsilon(\eta) = u_0(\eta) + \frac{1}{2}u_0''(\eta)\{1 - u_0(\eta)\}\epsilon + \{E_2(\eta) + o(1)\}\epsilon^2 \quad (A7)$$

where $E_2(\eta)$ is given by

$$E_2(\eta) = \int_{\eta}^{\infty} e^{-t^2/4} \int_0^t e^{s^2/4} f_\epsilon(s) ds dt - A_\epsilon \int_{\eta}^{\infty} e^{-t^2/4} dt \quad (A8)$$

In the latter expressions $f_\epsilon(\eta)$ and A_ϵ are

$$f_\epsilon(\eta) = (1 - 3u_0(\eta))(u_0'(\eta))^2 - u_0''(\eta) \int_{\eta}^{\infty} \{u_0'(s)\}^2 ds \quad (A9)$$

$$A_\epsilon = \frac{1}{2\sqrt{\pi}} \int_{-\infty}^{\infty} e^{-t^2/4} \int_0^t e^{s^2/4} f_\epsilon(s) ds dt \quad (A10)$$

Both series expansions are truncated after the ϵ^2 terms. A nice property of the approximate solutions u_ϵ and v_ϵ is that they are expressed in terms of the solution of the Boussinesq problem B_I and the small parameter ϵ only. Because $u_0(\eta)$ is known explicitly, u_ϵ and v_ϵ can be evaluated without great difficulty, for instance with the computer algebra package Maple¹⁹.

In the Boussinesq limit for Problem II we have again $v_0 = 0$ while now u_0 is the solution of

$$B_{II} \begin{cases} u_0'' + \frac{1}{2}\eta u_0' = 0 \text{ for } \eta > 0 \\ u_0(0) = 1 \text{ and } u_0(+\infty) = 0 \end{cases} \quad (A11)$$

hence

$$u_0(\eta) = \operatorname{erfc}\left(\frac{\eta}{2}\right) \quad (A12)$$

[†]The expression $f(x) = 0(\psi(x))$ for $x \rightarrow +\infty$ means that $f(x)/\psi(x)$ tends to zero when $x \rightarrow \infty$. It can be read as: 'Something that tends to zero, multiplied by'.

The asymptotic expressions for Problem II are

$$v_\varepsilon(\eta) = \left\{ \frac{(1-\gamma)}{\sqrt{\pi\gamma}} - u'_0(\eta) \right\} \varepsilon + \{E_3(\eta) + o(1)\} \varepsilon^2 \quad (\text{A13})$$

and

$$u_\varepsilon(\eta) = u_0(\eta) - \left\{ \frac{2(1-\gamma)}{\pi\gamma} \{u_0(\eta) + \sqrt{\pi}u'_0(\eta)\} + \frac{1}{2}u_0(\eta)\{1 - u_0(\eta)\} \right\} \varepsilon + \{E_4(\eta) + o(1)\} \varepsilon^2 \quad (\text{A14})$$

with

$$E_3(\eta) = \frac{\gamma^2 - \gamma + 1}{\sqrt{\pi\gamma}} + u'_0(\eta) \left(2u_0(\eta) - \frac{\gamma(\pi + 4) - 4}{2\gamma\pi} \right) - \frac{2(\gamma - 1)}{\gamma\sqrt{\pi}} u''_0(\eta) + \int_\eta^{+\infty} \{u'_0(s)\}^2 ds \quad (\text{A15})$$

and

$$E_4(\eta) = A_\varepsilon \int_0^\eta e^{-t^2/4} dt - \int_0^\eta e^{-t^2/4} \int_0^t e^{s^2/4} f_\varepsilon(s) ds dt \quad (\text{A16})$$

The function $f_\varepsilon(\eta)$ and the constant A_ε are defined as

$$f_\varepsilon(\eta) = \left(\frac{1}{2}u_0(\eta)(1 - u_0(\eta)) + \frac{2(\gamma - 1)}{\gamma\pi} (u_0(\eta) + \sqrt{\pi}u'_0(\eta)) \right) \left(u'_0(\eta) - \frac{1-\gamma}{\gamma\sqrt{\pi}} \right) - u'_0(\eta)E_3(\eta) \quad (\text{A17})$$

and

$$A_\varepsilon = \frac{1}{\sqrt{\pi}} \int_0^\infty e^{-t^2/4} \int_0^t e^{s^2/4} f_\varepsilon(s) ds dt \quad (\text{A18})$$